Research Square

Preprints are preliminary reports that have not undergone peer review.
They should not be considered conclusive, used to inform clinical practice,
or referenced by the media as validated information.

Schistosoma mansoni Infection Alters Antibody Subclass Profiles but Preserves SARS-CoV-2 mRNA Vaccine-Induced Neutralizing Activity in a Murine Model

Yi Mu
QIMR Berghofer Medical Research Institute
Kexin Yan
QIMR Berghofer Medical Research Institute
Cameron Bishop
QIMR Berghofer Medical Research Institute
Daniel J. Rawle
QIMR Berghofer Medical Research Institute
Malcolm K. Jones
University of Queensland
Pengfei Cai
Pengfei.Cai@qimrberghofer.edu.au

QIMR Berghofer Medical Research Institute https://orcid.org/0000-0003-4975-4615

Research Article

Keywords: Schistosoma mansoni, helminth infection, SARS-CoV-2, BNT162b2, mRNA vaccination, antibody subclasses, neutralizing assay, vaccine immunogenicity

Posted Date: November 12th, 2026

DOI: https://doi.org/10.21203/rs.3.rs-11695106/v1

License: This work is licensed under a Creative Commons Attribution 4.0 International License.
Read Full License

Additional Declarations: The authors declare no competing interests.

Abstract

Objectives

Helminth infections can modulate host immune responses and potentially influence immunogenicity of vaccines against unrelated pathogens. This study investigated the effects of *Schistosoma mansoni* infection on immune responses to COVID-19 mRNA vaccine (BNT162b2) on in a murine model.

Methods

Two experiments were conducted using C57BL/6J mice assigned to three groups: uninfected and unvaccinated controls, *S. mansoni*-infected vaccinated mice, and uninfected vaccinated mice. The experiments differed in parasite inoculum and BNT162b2 vaccine dose. IgG, IgG1, and IgG2a antibodies against the spike-protein S1 were measured by enzyme-linked immunosorbent assay (ELISA). SARS-CoV-2 neutralizing activity was assessed using an *in vitro* virus neutralization assay. For Experiment 1 (Exp 1), bulk RNA sequencing (RNA-seq) of spleen tissues and measurement of cytokine production by peptide-stimulated splenocytes were also performed.

Results

Vaccination induced robust spike-specific antibody responses in both infected and uninfected mice. In Exp 1, infected mice exhibited significantly higher total IgG and IgG2a titres than uninfected vaccinated mice following the booster dose. In Experiment 2 (Exp 2), antibody titres were comparable between vaccinated groups. The IgG2a/IgG1 ratio was consistently higher in uninfected vaccinated mice, suggesting that *S. mansoni* infection altered vaccination-induced antibody subclass profiles. In Exp 1, liver egg burden was inversely correlated with IgG2a titres (Spearman's $\rho = -0.87$, $p = 0.0054$), but this association was not observed in Exp 2. Peptide-stimulated splenocytes from infected mice showed significantly lower levels of the Th1-associated cytokines in infected mice. Despite these immunological changes, neutralizing activity did not differ significantly between infected and uninfected vaccinated mice in either experiment. Neutralizing titres were positively correlated with total spike-specific IgG and IgG2a titres in both experiments.

Conclusions

S. mansoni infection modified Th1-associated immune response to BNT162b2 vaccination, particularly antibody subclass distribution, without consistently reducing spike-specific antibody titres or SARS-CoV-2 neutralizing activity. These findings suggest that helminth-associated immune modulation can alter vaccine-induced immune responses without necessarily compromising the generation of functional antiviral antibodies. Further studies involving direct viral challenge and longer-term immune

assessments are needed to determine whether these responses confer equivalent protection in infected and uninfected hosts.

1. Introduction

Severe acute respiratory syndrome coronavirus 2 (SARS-CoV-2), a virus emerging in late 2019 causing coronavirus disease 2019 (COVID-19), resulted in an unprecedented global crisis. SARS-CoV-2 initiates infection through binding to the angiotensin-converting enzyme (ACE) 2 receptors by the viral S (spike) protein receptor-binding domain (RBD). Infection triggers a Th1 response, which is characterised by increased levels of the pro-inflammatory cytokines, TNF-α, interleukin (IL)-2 and IL-6 in plasma (1, 2). When uncontrolled, the massive release of pro-inflammatory cytokines leads to a cytokine storm (3), which is positively associated with the severity of the viral infection and mortality rate. In terms of pathogenesis and understanding the disease mechanism, accumulating evidence shows that viral sepsis is a crucial process in critically ill patients with COVID-19 (4). The pandemic has also led to a rapid development and deployment of novel vaccines for the SARS-CoV-2 virus. The most effective COVID-19 vaccines (i.e., Pfizer, Moderna and AstraZeneca) mount a Th1-skewed immune response (5).

Parasitic helminths, including roundworm (*Ascaris lumbricoides*), whipworm (*Trichuris trichiura*), and hookworm (*Necator americanus*, *Ancylostoma duedenale*), collectively known as soil-transmitted helminths, and the schistosome bloodflukes are among the most common infectious disease agents, afflicting over 1.8 billion people globally (6), particularly those living in low- and middle-income countries (LMICs) (7). It is well documented that hosts chronically infected with helminths typically elicit an anti-inflammatory Th2 immune response, which is characterized by the activation of Th2 cells and the elevation of IL-4, IL-5, IL-9, IL-10, IL-13, IgE, TGF-β, mast cells, eosinophils and M2 macrophages (8–10). However, the regulatory response initiated by chronic helminth infection was also important in downmodulating immune responses and pathology by actively inducing the expansion of $FOXP^{3+}$ regulatory T cells (Tregs), IL-10 producing B cells (Bregs) and alternatively activated macrophages (AAMs), which together promote the release of regulatory cytokines such as TGF-β and IL-10 (11–14). This host-helminth interaction could be beneficial in dampening inflammatory damage induced by the Th1/Th17 branches of the immune system, repairing injured tissue and restoring homeostasis(15). In addition, there are published claims that a concurrent helminth infection could reduce human immune responses to vaccines against other types of pathogens including bacteria, viruses and protozoa (16–18), in which immunosuppression occurs through the involvement of interleukin (IL)-10 and type 1 regulatory T cells (Tr1) (17). In contrast, others found helminth infection had no influence on vaccine responsiveness in humans (19, 20).

Given the likelihood of co-occurrence of SARS-CoV-2 infection and pre-existing helminth infections in many low-middle income countries (LMICs), it is important to investigate how helminth-induced immunomodulation may influence the immunogenicity and efficacy of COVID-19 vaccines. Addressing this knowledge gap could inform the development and deployment of novel vaccines and vaccination strategies in LMICs. In 2022, a call has been made for the scientific research communities and funders

to support clinical trials of full, fractional, and booster doses of COVID-19 vaccine in people with helminth infections, a population representing one-quarter of humanity (21). Although several studies using murine models have investigated the effects of helminth infections on COVID-19 vaccine-induced immune responses, their findings have been inconsistent (22, 23). However, the extent to which pre-existing helminth infections influence the immunogenicity of COVID-19 vaccines in vaccinated human populations, as well as the underlying immunological mechanisms, remains poorly understood (24, 25).

In our previous human cohort study in helminth-endemic villages in Mayuge District, Uganda, we found that moderate-to-heavy *S. mansoni* infection was associated with reduced anti-spike IgG responses following mRNA COVID-19 vaccination (25). To investigate potential mechanisms underlying this observation, in this study, we examined the effects of *S. mansoni* infection on BNT162b2 vaccine responses in a murine model under two experimental conditions that differed in parasite inoculum, vaccine dose and final assessment time point. The blood fluke, *S. mansoni*, is a well-characterized parasitic helminth species that elicits a Th2-skewed immune response during a chronic infection following egg deposition.

2. Methods

2.1. Animals, immunization, and live SARS-CoV2 challenge

Two animal experiments were carried out, each comprising three groups of C57BL/6J mice [Group 1: uninfected and unvaccinated mice served as the control group; Group 2: mice infected with *S. mansoni* and subsequently vaccinated with SARS-CoV-2 BNT162b2 mRNA vaccine (Pfizer BioNTech); and Group 3: un-infected mice vaccinated with BNT162b2]. In experiment 1 (Exp 1, n = 8 mice per group), mice in Group 2 were anaesthetized with ketamine (100 mg/kg) and Xylazin-20 (20 mg/kg) prior to percutaneous challenge to *S. mansoni* cercariae (low number, 15 ± 5). At 8 weeks post infection (p.i.), Group 2 and 3 were immunized with two doses of BNT162b2 (1 µg/mouse, with a volume less than 0.05 ml per site) administered at an interval of 3 weeks. Group 1 mice received two doses of PBS as control. Three weeks after the second vaccination, the animals were euthanized and liver and spleen tissues were collected for further assessment. Blood samples were collected before infection, 2 weeks after the first vaccination dose and 3 weeks after second vaccination dose.

Experiment 2 (Exp 2, n = 10 per group) followed a similar experiment design, with following modifications. First, Group 2 mice were infected with a higher number of schistosome cercariae (30 ± 2) compared with that in Exp 1. Second, mice in Group 2 and 3 received a relatively low dose of BNT162b2 (0.2 µg/mouse). Third, the animals were euthanized 1 week after the booster immunisation.

2.2. Liver egg counts

Liver egg counts were performed to determine the number of eggs per gram (EPG) in the liver as a measure of infection burden (26). Briefly, a weighed portion of liver tissue was digested overnight at

37°C with 5% (w/v) KOH. The homogenate was centrifuged at 2000 × *g* for 10 min, washed with 5% KOH (w/v). The pellet containing eggs was resuspended in 2 mL of 4% (v/v) formalin for fixation. Eggs were counted in three 10-µL aliquots, and the egg numbers were averaged to calculate the mean eggs per gram (EPG) of liver.

2.3. ELISA

Anti-SARS-CoV-2 antibody titers were measured by enzyme-linked immunosorbent assay (ELISA), as previously described, (25) with modification. Briefly, SARS-CoV-2 Spike Protein S1 (amino acids 14–683) (Cat# RP87681; Thermo Fisher Scientific) was coated onto Max-absorb 96-well plates (Nunc, Thermo Fisher Scientific, USA) at a concentration of 1 µg/mL in coating buffer (100-µL per well) and incubated overnight at 4°C. Following removal of the coating solution, the wells were blocked with 150 µl of blocking buffer [1% BSA in 1× PBST (phosphate-buffered saline and 0.05% Tween-20)] at 37°C for 1 h. Serial two-fold dilutions of sera were prepared and added to each well (100 µL per well) followed by incubation at 37°C for 1 h. After removal of the diluted sera, a biotin-SP-conjugated goat anti-mouse IgG (Fcγ specific) antibody (Jackson ImmunoResearch Labs, PA, USA) was added as a secondary antibody (1:20,000, 100 µL/well) and incubated at 37°C for 1 h. The plates were then incubated with streptavidin-HRP (Cat# 554066, BD Biosciences, CA, USA) at a 1:10,000 dilution (100 µL/well) for 30 min. The plates were washed 5 times with wash buffer after each step following the addition of serum. TMB substrate (100 µL/well; Cat# 860336, Merck Life Science, Australia) was then added, and the reaction was terminated by adding 50 µL of stop solution (2 N H_2SO_4). The optical density (OD) was measured at 450 nm using an Infinite M Nano plate reader (Tecan, Männedorf, Switzerland).

To assess the titers of IgG subclasses (IgG1 and IgG2a) against the SARS-CoV-2 S1 protein in serum, a similar protocol was followed, except that different second antibodies were used and without the step of streptavidin-HRP incubation. Horseradish peroxidase (HRP)-conjugated secondary antibodies specific to mouse Goat anti-Mouse IgG1 Cross-Adsorbed Secondary Antibody, HRP (Catalog: A10551, Thermo Fisher Scientific, AU) and Goat anti-Mouse IgG2a Secondary Antibody, HRP (Catalog: A10685 Thermo Fisher Scientific, AU) were used at a 1:2,000 dilution.

2.4 Spleen cell preparation and stimulation

Splenocytes were isolated by gently pressing the spleen through a 70-µm cell strainer to produce a single cell suspension. Red blood cells were removed using RBC lysis buffer (Thermo Fisher Scientific, AU), after which the cells were washed and resuspended in Iscove's Modified Dulbeccco's Medium (IMDM; Thermo Fisher Scientific, AU). The purified splenocytes were counted, and cell viability was assessed using the Trypan blue exclusion method. Cells were seeded in 96 well plates (10^7 cells/mL, 150 µl/well) and stimulated with PepTivator according to the manufacturer's instructions. Peptide pools were used at a final concentration approximately 1 µg/mL of each peptide. Concanavalin A (Con A) stimulation at 1 µg/mL was utilized as a positive control. Cell culture supernatants were collected 6 h after stimulation. The cytokine concentrations were measured using LEGENDplex MU Th1/Th2 Panel (8-plex) w/VbP V03 kit according to the manufacturer's instructions. Data were acquired using a flow

cytometer (Beckman Coulter, USA) and analyzed using the online LEGENDplex Data Analysis Software Suite.

2.5. SARS-CoV-2 neutralization assay

Neutralization assay was carried out as described (27). Briefly, mouse serum was heat-inactivated at 56°C for 30 min and serially diluted 2-fold. Aliquots of each serum dilution (50 µl) were incubated with 100 $CCID_{50}$ SARS-CoV-2 (50 µl, Wuhan strain) for 1 h at 37°C in round bottom 96 well plates containing RPMI1640 supplemented with 2% fetal calf serum (FCS), penicillin, streptomycin and L-glutamine. The serum-virus mixtures were then added to wells of 96 well plates containing 10^5 Vero E6 cells in 100 µl of medium supplemented with 10% FCS. After 5 days, cells were fixed and stained by adding 50 µl of formaldehyde (15% w/v) and crystal violet (0.1% w/v; Sigma-Aldrich) overnight. The plates were washed with tap water and dried overnight, after which 100% methanol (100 µl/well) was added to dissolve the crystal violet. Optical density (OD) was measured at 595 nm using a 96-well plate reader (Biotek Synergy H4). The 50% neutralizing titers were interpolated from plots of OD versus serum dilution. The OD of wells containing cells and serum in the absence of virus was defined as 100% neutralization (0% CPE), whereas the OD observed from wells containing cells, virus and naïve control serum was defined as 0% neutralization (> 80% CPE).

2.6. Bulk RNA-seq of spleen tissue and bioinformatics analysis

RNA-seq and bioinformatic analyses of differential gene expression (DGE) in spleen tissue among the different groups were undertaken as described (28, 29). Briefly, total RNA was extracted from spleen tissues using TRIzol reagent. RNA concentration and quality were assessed using D1000 TapeScreen assay (Agilent Technologies, Santa Clara, USA). cDNA libraries were constructed using the Illumina TruSeq stranded mRNA library preparation kit (Illumina, San Diego, USA) to generate NGS Library amplicons which were further sequenced on the NextSeq 2000 platform (Illumina, San Diego, USA) to generate 100-bp single-end reads. Per-base sequence quality was assessed and > 90% bases had a quality score above Q30 in all samples. The quality of raw sequencing datasets was assessed using FastQC (30) (v0.11.8). Sequence reads were trimmed to remove adapter sequences using Cutadapt version 1.9 (Martin (2011). Trimmed reads were aligned to the GRCm39 assembly with the gene, transcript, and exon features of Ensembl release v109 gene model using STAR (v2.5.2a). Quality-control metrics were calculated using RNA-SeQC version 1.1.8. Mouse gene expression levels were estimated using RSEM (v1.2.30) (31). DGE among different groups was analyzed using EdgeR (3.22.3), with the likelihood ratio test implemented in glmLRT. Principal component analysis (PCA) was performed on normalized gene expression data to assess overall transcriptional variation among spleen samples from the three experimental groups. The expression data were transformed and subjected to PCA, and the first two principal components (PC1 and PC2) were plotted to visualize sample clustering and differences in gene expression profiles between groups. For volcano plots generation, genes were considered significantly differentially expressed if they had an adjusted *p* value (padj) < 0.05 and a

$\log_2^{\text{Fold Change}}$ greater than 1. The differentially expressed genes (DEGs) between the infected, vaccinated group and the non-infected, vaccinated group, were analysed using Ingenuity Pathway Analysis (IPA, v84978992, QIAGEN) (32).

2.7 Statistical analysis

Data analysis and visualization were performed using GraphPad Prism (v.11) for windows (GraphPad Software, Inc., San Diego, CA, USA) and SRplot (33). Results are expressed as the arithmetic means ± SEM. For antibody titers, the log-transformation data were used. Mann-Whitney *U* test, Kruskal-Wallis test followed with Dunn's multiple comparisons test (25) or One-way ANOVA test followed by Turkey's comparison was employed to detect significant differences between different groups. Correlations between variables were determined by Pearson's or Spearman's correlation coefficient. Data comparison with a p value < 0.05 was considered statistically significant.

3. Results

3.1 Humoral responses to COVID-19 mRNA vaccination in Exp 1

At the termination of Exp 1, liver egg burdens in the infected group ranged from 9,109 to 32,051 eggs per gram of liver (EPG), with a mean of 19,843 EPG (Fig. S1A). To investigate the effects of *S. mansoni* infection on humoral responses to COVID-19 mRNA vaccination, spike-specific antibody responses were assessed in infected and uninfected mice following immunization. *S. mansoni*-infected mice had significantly larger spleens than uninfected mice (Fig. 2A, B). Vaccination induced robust anti spike S1-specific IgG responses, which increased significantly following the booster immunization in both infected and uninfected mice (Fig. 2C, D).

Following the first dose, mRNA vaccinations induced similarly high spike-specific IgG, IgG1, and IgG2a titers in *Sm*-infected and non-infected mice, with no difference in the IgG2a/IgG1 ratio (Fig. 2E). Following the second dose, mRNA vaccinations induced significantly high IgG (p = 0.0427) and IgG2a (p = 0. 0030) titers in *Sm*-infected mice compared with non-infected mice (Fig. 2F). Notably, vaccinated non-infected mice had a higher IgG2a/IgG1 ratio compared with non-infected vaccinated mice. SARS-CoV-2 spike-specific IgG, IgG1 and IgG2a were undetectable in unvaccinated non-infected mice (Fig. 2E, F). No correlations were observed between liver egg burden and IgG, IgG1, and IgG2a/IgG1 ratios (Fig. 2G). However, a significant inverse correlation was observed between liver egg burden and IgG2a titres (Spearman's $\rho = -0.87$, p = 0.0054; Fig. 2G)

3.2 Cytokine responses to COVID-19 mRNA vaccination of Exp 1

Beyond the antibody responses, peptide stimulated cells induced robust production of IFN-γ, IL-2, TNF-α, and IL-5, as well as up-regulation of IL-6 and IL-13 in the BNT162b2 vaccination groups. In contrast, low levels of the Th2-associated cytokines, IL-4 and IL-10, were detected. Splenocytes from *Sm*-infected mice tended to produce lower levels of Th1-associated cytokines IFN-γ, TNF-α, and IL-2 following peptide stimulation (Fig. 3A-C). However, no significant difference was observed in the production of IL-6, IL-5, IL-4, IL-10, and IL-13 (Fig. 3D-H).

3.3 Neutralizing assay of Exp 1

At three weeks after the second immunization, both vaccination groups showed comparable levels of SARS-CoV-2 virus neutralizing activity for IC50 (Fig. 4A). Neutralizing antibody titres showed a negative correlation with liver egg burden but did not reach a statistical significance (Pearson's r = − 0.65, p = 0.078; Fig. 4B). When data from both vaccinated groups were combined, neutralizing antibody titres (IC50) were significantly positively correlated with total IgG titres (Spearman's ρ = 0.81, p = 0.00016) and IgG2a titres (Spearman's ρ = 0.63, p = 0.0087) (Fig. 4C). In contrast, no significant correlation was observed between neutralizing antibody titres and IgG1 titres (Spearman's ρ = 0.28, p = 0.3) (Fig. 4C).

3.4 Bulk RNA-seq of spleen tissue

Bulk RNA-seq analysis of spleen tissue revealed distinct transcriptional profiles in infected, vaccinated mice (G2) compared with non-infected PBS controls (G1) and non-infected, vaccinated mice (G3), as shown by principal component analysis (PCA; Fig. 5A). A total of 653 differentially expressed genes (DEGs) were identified between infected, vaccinated and non-infected, vaccinated mice (G2 vs G3, 606 upregulated, and 47 downregulated), while 674 DEGs were identified between infected, vaccinated mice and non-infected PBS controls (G2 vs G1, 629 upregulated, and 45 downregulated), (Fig. 5B). No DEGs were identified between the non-infected, vaccinated and non-infected PBS control groups (Fig. 5B). The two infection-associated comparisons showed substantial overlap in both upregulated (88.4%) and downregulated (61.4%) DEGs (Fig S2), suggesting that *S. mansoni* infection was the major driver of the observed transcriptional changes, irrespective of vaccination status. Ingenuity Pathway Analysis (IPA) of DEGs between infected, vaccinated (G2) and non-infected, vaccinated (G3) mice predicted enhanced immune-related activity and cell proliferation in G2 (Ingenuity Canonical Pathways) (Fig. 3C). The Diseases and Functions analysis further indicated activation of processes associated cellular movement, migration, survival, viability, and invasion in G2 (Fig. 5D). Cytokine upstream regulator analysis did not indicate a clear Th2-biased response. Instead, both Th1- and Th2-associated cytokines were represented, with prominent signals involving colony-stimulating factors (CSFs) (Fig. 5E).

3.5 Humoral responses to COVID-19 mRNA vaccination of Exp 2

In Exp 2, mice in Group 2 were infected with a higher number (compared with the Exp 1) of *S. mansoni* cercariae (30) but immunized with a lower dose of (0.2 μg) mRNA vaccine. The final analysis was

performed 1 week after the boost immunization. At termination of the experiment, 6 out of 10 mice were successfully infected in Group 2, showing liver egg burden between 17,337 and 34,135 EPG, with a mean EPG of 25,852 (Fig. S1B). Similar to the observation in Exp 1, *Sm*-infected mice showed significant longer and heavier spleens compared with un-infected groups (Fig. 6A, B). Vaccinated groups induced robust spike-specific IgG, with significantly increased IgG response following the boost immunisation in both *Sm*-infected and non-infected mice ($p = 0.0260$, and $p < 0.0001$, respectively) (Fig. 6C, D). Following the first and boost dose, there were no difference in spike S1-specific IgG, IgG1, and IgG2a titers in *Sm*-infected and non-infected mice ($p > 0.05$), although there is a trend that IgG2a titers were lower in *Sm*-infected mice than non-infected mice ($p = 0.0668$) (Fig. 6E, F). However, mRNA vaccinations induced significantly higher IgG2a/IgG1 ratio in non-infected mice compared with *Sm*-infected mice (Fig. 6F). Unvaccinated non-infected mice did not induce undetectable SARS-CoV-2 spike-specific IgG, IgG1 and IgG2a responses (Fig. 6E, F). No correlations were observed between liver egg burden and IgG, IgG1, and IgG2a titres as well as IgG2a/IgG1 ratios (Fig. 6G).

3.6 Neutralizing assay of Exp 2

At 1 week after the second immunization, there was no difference in SARS-CoV-2 virus neutralizing titer (IC_{50}) between *Sm*-infected and non-infected vaccination groups ($p = 0.4740$) (Fig. 7A). There was no correlation between the neutralizing antibody titres with liver egg (Spearman's $\rho = 0.12$, $p = 0.83$; Fig. 7B). When data from both vaccinated groups were combined, neutralizing antibody titres (IC50) were significantly positively correlated with total IgG titres (Spearman's $\rho = 0.66$, $p = 0.0051$), IgG1 titres (Spearman's $\rho = 0.53$, $p = 0.033$) and IgG2a titres (Spearman's $\rho = 0.67$, $p = 0.0047$) (Fig. 7C).

4. Discussion

Helminths are potent immunomodulators that can skew or impair host immune responses to unrelated antigens, including those derived from viruses and vaccines (18, 34). In this study, we investigated the impact of *S. mansoni* infection on the immunogenicity of the BNT162b2 mRNA COVID-19 vaccine using two experimental settings that differed in parasite inoculum and vaccine dose, and final assessment time point. Overall, our findings indicate that *S. mansoni* infection did not consistently impair the magnitude of vaccine-induced spike-specific antibody responses. No significant differences in antibody titres were observed between infected and non-infected groups following the first vaccine dose. However, following the booster dose in Exp 1, *S. mansoni*-infected mice exhibited significantly lower total IgG and IgG2a titres than uninfected vaccinated mice. In contrast, antibody titres tested were comparable between the vaccinated groups in Exp 2, despite the higher parasite burden in Group 2 compared with that in Exp 1. The findings from Exp 2 thus were consistent with those of Su et al (35), who reported no significant differences in IgG responses were observed between infected and non-infected mice immunized with 1 μg or 5 μg mRNA vaccine and accessed one week after second booster immunisation. The discrepancy between Exp 1 and Exp 2 may reflect variation in the timing of immune assessment and the immunological context of infection. Nevertheless, the finding in the Exp 1 were consistent with our previous observations in a Ugandan human cohort, in which anti-S1 IgG titres were

significantly lower in subjects with moderate or heavy *S. mansoni* infection than in those who tested negative by the Kato-Katz method (25). One possible explanation for the reduced vaccine-induced humoral response is that *S. mansoni* infection affects the persistence of vaccine-induced antibodies rather than their initial induction. This possibility is supported by Musaigwa et al (36), who demonstrated that chronic *S. mansoni* infection induces plasmablast and plasma cell death in the bone marrow, potentially accelerating the decline of vaccine-induced antibody responses. Longitudinal studies measuring antibody titres at multiple time points following vaccination are therefore needed to determine whether *S. mansoni* infection accelerates the waning of vaccine-induced humoral responses in vaccinated hosts.

Although infection did not consistently suppress total IgG production at time points measured, antibody subclass profiles suggested differences in humoral immune responses. Particularly, the IgG2a/IgG1 ratio was constantly lower in infected vaccinated mice than in uninfected vaccinated mice in both experiments, indicating an impaired anti-viral Th1 response in *Sm*-infected mice, although IgG2c/IgG1 ratio would be a more appropriate measure for C57BL/6J mice (37, 38). In Exp 1, liver egg burden was also negatively correlated with IgG2a titres, suggesting that animals with greater parasite burdens tended to have lower spike S1-specific IgG2a response. However, this association was not observed in Exp 2. This divergence should be interpreted cautiously given the small sample sizes and variability in experimental design, including earlier assessment of humeral responses following booster immunisation and a narrower range of liver egg burdens in Exp 2. Nevertheless, the findings from Exp 1 raise the possibility that infection burden may influence specific components of the Th1-associated antibody response elicited by the mRNA vaccine.

Our cytokine analyses provided additional evidence of potential immune modulation. Peptide-stimulated splenocytes from both infected mice and uninfected vaccinated mice were assessed for cytokine production as a measure of antigen-specific recall responses. Compared with uninfected vaccinated mice, splenocytes from infected mice tended to produce lower levels of IFN-γ, TNF-α, and IL-2, suggesting potential attenuation of selected Th1-associated recall responses. No significant differences were observed in the other measured cytokines, including IL-4 and IL-5. These findings suggest no generalized shift towards a Th2-dominant response. As cytokine concentrations in culture supernatants do not directly establish changes in antigen-specific T-cell frequency or function, further cellular characterization is needed to clarify these observations. Interestingly, our findings are consistent with those of Su et al (22), who reported that *S. mansoni* infection modulated the immunogenicity of COVID-19 mRNA vaccines in mice, resulting in reduced frequencies and polyfunctionality of vaccine-specific $CD8^+$ T cells, despite relatively preserved $CD4^+$ T-cell and antibody responses. Given the contributions of Th1-associated responses and cytotoxic $CD8^+$ T cells to antiviral immunity of mRNA vaccines (39), the observed reduction in Th1-associated recall cytokines in our study may be immunologically and clinically relevant. Although the present data do not establish reduced protective immunity based on the neutralizing assays, the observed tendency towards lower Th1-associated cytokine production and IgG2a/IgG1 ratio warrants further investigation to determine whether infection alters vaccine-induced cellular immune memory.

Importantly, the impaired Th1-associated immune responses, evidenced by lower IgG2a/IgG1 ratios and reduced levels of Th1-associated cytokines, were not accompanied by significant reduction in SARS-CoV-2 neutralizing activity, consistent with the findings of Su et al (22). In that study, *Sm*-infected and non-infected mice were immunized with the Comirnaty (Pfizer-BioNTech) COVID-19 vaccine at 4-week intervals, and protective efficacy was assessed using neutralizing assays and SARS-Cov-2 challenge. In the present study, neutralizing titres were comparable between infected and uninfected vaccinated mice in both experiments. These results indicate that the changes in antibody composition observed in Exp 1 did not translate into a detectable reduction in neutralizing activity against the Wuhan strain under the conditions tested, i.e., 3 weeks following the booster dose and with the current sample size. However, neutralizing titres were prone to be positively correlated with total spike-specific IgG and IgG2a, compared with IgG1 subclass, suggesting a potential association between Th1-biased antibody responses and vaccine-induced neutralizing activity (40). Notably, liver egg burden showed a negative correlation with neutralizing titres in Exp 1, although this association did not reach statistical significance ($p = 0.078$; Fig. 4B). In both experiments, the primary immunisation was administered 8 weeks after *S. mansoni* infection, when the host immune response is typically within the post-patent acute phase, generally spanning weeks 5–12 and characterized by a strong Th2-dominant immune profile (41). By the time of the booster dose, the host response to *S. mansoni* may have begun transitioning toward a more regulated immune state, preceding the down-modulation of Th2 responses associated with the chronic phase (12 weeks post-infection onward). This transition is thought to be primarily mediated by IL-10 (41, 42), consistent with the predicted involvement of IL-10 in our upstream regulator analysis (Fig. 5E). These infection-associated changes in immune regulation may help explain why *S. mansoni* infection did not result in a significant reduction in SARS-CoV-2 neutralizing activity in vaccinated mice. Further studies assessing neutralizing activity and cellular immune responses at multiple time points across a wider range of infection burdens and vaccine doses would help clarify the relationship between parasite burden and vaccine-induced immunity and its potential clinical significance.

Bulk RNA-sequencing (bulk RNA-seq) detected splenic DEGs between *S. mansoni*-infected and non-infected groups. It failed to detect significant DEGs three weeks after the second dose immunisation between non-infected vaccinated and non-infected non-vaccinated mice, potentially due to systemic innate immune activation has largely subsided (43), while persistent adaptive immune responses may be restricted to antigen-specific cells (e.g., germinal center B cells or memory T cells) (44). Bulk RNA-seq captures the average expression profile of the entire tissue sample. Because these antigen-specific constitute a minute percentage of the total splenic mass, their specific, localized transcriptomic changes are completely overwhelmed and obscured by the background RNA of billions of inactive bystander cells. Single-cell RNA-seq, spatial transcriptomics, or targeted analyses of sorted immune populations may provide greater resolution for investigating persistent splenic immune responses and vaccine-induced immune memory (45, 46).

This study provides experimental evidence that complements previous findings from human cohort studies (24, 25). In our study, *S. mansoni*–infected mice maintained comparable serum neutralizing

activity compared with non-infected group, consistent with findings from other experimental studies (35). These results suggest that the reduced anti-spike IgG observed in vaccinated adolescents with moderate-to-heavy *S. mansoni* infection (25) do not necessarily imply impaired protective efficacy. However, it should be noted that experimental infections in mice cannot fully reproduce the immune responses in naturally acquired schistosomiasis or other helminth infections in humans occur within a complex immunological and epidemiological context, such as repeated infections, co-infections, and anthelmintics treatment. Notably, a recent cross-sectional study in Malawi found that helminth infection was associated with reduced neutralizing antibody responses following COVID-19 vaccination, but not following natural SARS-CoV-2 infection, as assessed using a human immunodeficiency virus (HIV)-based pseudotyped virus neutralization assay (24). Future studies should investigate a broader range of parasite burdens, assess the durability and breadth of antibody responses, and directly evaluate protective efficacy by SARS-CoV-2 challenge. Integrating experimental models with longitudinal human studies will be essential to determine the mechanisms underlying reduced vaccine immunogenicity in helminth-endemic populations.

The study has several limitations. First, the relatively small sample sizes limit statistical power to detect modest differences and reduce the reliability of correlation analyses. Second, immune responses were assessed at selected time points, and the durability of antibody responses and the development of long-lived plasma cells and memory lymphocytes were not determined. Third, cellular immunity was assessed primarily through cytokine measurements rather than direct characterization of antigen-specific lymphocyte populations.

5. Conclusion

In conclusion, this study demonstrates that *S. mansoni* infection can modulate certain aspects of BNT162b2 mRNA COVID-19 vaccine-induced immunity, including antibody subclass profiles and Th1-associated cytokine responses, without consistently reducing spike-specific antibody titres or SARS-CoV-2 neutralizing activity. Although infected mice exhibited lower IgG2a/IgG1 ratios and trends towards reduced production of Th1-associated cytokines, these alterations were not accompanied by a detectable impairment in neutralizing activity against the Wuhan strain under the conditions investigated. Further studies incorporating longitudinal assessments, detailed characterization of antigen-specific B- and T-cell responses, and direct evaluation of protective efficacy are warranted. Collectively, these findings suggest that schistosomiasis may alter the quality of vaccine-induced immune responses without necessarily compromising functional antibody activity, underscoring the need to investigate the long-term implications of helminth infection for vaccine-induced immune memory and protection in human populations.

Declarations

Data availability statement

The data supporting the findings of this study are available from the corresponding authors upon reasonable request. The RNA sequencing data have been deposited in the NCBI Sequence Read Archive (SRA) under accession number PRJNA1559204.

Ethics Statement

All animal work was conducted with the approval of the QIMR Berghofer Animal Ethics Committee (Project ID: P3818). All animal studies were performed according to the Australian Code for the Care and Use of Animals for Scientific Purposes (8th edition).

Authors' contributions

PC formulated the research aims and prepared the study protocol. PC supervised the research. DJR, MKJ, and PC provided study materials. YM, KY, CB, DJR and PC developed the methodology, collected and analyzed the data. PC drafted the original manuscript. YM, KY, CB, DJR, MKJ and PC critically reviewed and edited the manuscript. The authors read and approved the final manuscript.

Acknowledgements

We thank the National Institute of Allergy and Infectious Diseases (NIAID) Schistosomiasis Resource Center of the Biomedical Research Institute (Rockville, MD) for providing *Oncomelania hupensis quadrasi* (Möllendorff) snails (NIH-NIAID Contract HHSN272201700014I) through BEI Resources. We thank Mary Duke at the QIMR Berghofer for maintaining the *S. mansoni* life cycle. We appreciate Prof Andreas Suhrbier at the QIMR Berghofer for his help in the bioinformatic analysis and critical review of the manuscript.

Funding

This work was supported by an Australian Infectious Disease Research Centre Seed Grant, a QIMR Berghofer Seed Grant and grants APP2008433 and APP1194462 from the National Health and Medical Research Council (NHMRC) of Australia. This research was also funded by philanthropic donations for COVID-19 research from the Brazil Family Foundation, Australia. The funders had no role in the study design, data collection and analysis, decision to publish, or preparation of the manuscript.

Declaration of Competing Interests

The authors have no conflict of interest to declare.

References

1. Del Valle DM, Kim-Schulze S, Huang HH, Beckmann ND, Nirenberg S, Wang B et al (2020) An inflammatory cytokine signature predicts COVID-19 severity and survival. Nat Med 26(10):1636–1643

2. Huang C, Wang Y, Li X, Ren L, Zhao J, Hu Y et al (2020) Clinical features of patients infected with 2019 novel coronavirus in Wuhan, China. Lancet 395(10223):497–506
3. Ragab D, Salah Eldin H, Taeimah M, Khattab R, Salem R (2020) The COVID-19 Cytokine Storm; What We Know So Far. Front Immunol 11:1446
4. Li H, Liu L, Zhang D, Xu J, Dai H, Tang N et al (2020) SARS-CoV-2 and viral sepsis: observations and hypotheses. Lancet 395(10235):1517–1520
5. Dai L, Gao GF (2021) Viral targets for vaccines against COVID-19. Nat Rev Immunol 21(2):73–82
6. Disease GBD, Injury I, Prevalence C (2017) Global, regional, and national incidence, prevalence, and years lived with disability for 328 diseases and injuries for 195 countries, 1990–2016: a systematic analysis for the Global Burden of Disease Study 2016. Lancet 390(10100):1211–1259
7. Hotez PJ, Kamath A (2009) Neglected tropical diseases in sub-saharan Africa: review of their prevalence, distribution, and disease burden. PLoS Negl Trop Dis 3(8):e412
8. Harris NL, Loke P (2017) Recent Advances in Type-2-Cell-Mediated Immunity: Insights from Helminth Infection. Immunity 47(6):1024–1036
9. Abdoli A, Ardakani HM (2020) Helminth infections and immunosenescence: The friend of my enemy. Exp Gerontol 133:110852
10. Girgis NM, Gundra UM, Loke P (2013) Immune regulation during helminth infections. PLoS Pathog 9(4):e1003250
11. Turner JD, Jackson JA, Faulkner H, Behnke J, Else KJ, Kamgno J et al (2008) Intensity of intestinal infection with multiple worm species is related to regulatory cytokine output and immune hyporesponsiveness. J Infect Dis 197(8):1204–1212
12. Maizels RM, Yazdanbakhsh M (2003) Immune regulation by helminth parasites: cellular and molecular mechanisms. Nat Rev Immunol 3(9):733–744
13. Girgis NM, Gundra UM (2013) Loke Pn. Immune Regulation during Helminth Infections. PLoS Pathog 9(4):e1003250
14. Mu Y, McManus DP, Hou N, Cai P (2021) Schistosome Infection and Schistosome-Derived Products as Modulators for the Prevention and Alleviation of Immunological Disorders. Front Immunol 12:619776
15. Allen JE, Maizels RM (2011) Diversity and dialogue in immunity to helminths. Nat Rev Immunol 11(6):375–388
16. Nono JK, Kamdem SD, Musaigwa F, Nnaji CA, Brombacher F (2022) Influence of schistosomiasis on host vaccine responses. Trends Parasitol 38(1):67–79
17. Bullington BW, Klemperer K, Mages K, Chalem A, Mazigo HD, Changalucha J et al (2021) Effects of schistosomes on host anti-viral immune response and the acquisition, virulence, and prevention of viral infections: A systematic review. PLoS Pathog 17(5):e1009555
18. Yunus MS, Addo MM, Breloer M, Hartmann W (2026) The forgotten variable in vaccine immunology: helminth infection. Trends Parasitol 42(5):390–407

19. Wajja A, Kizito D, Nassanga B, Nalwoga A, Kabagenyi J, Kimuda S et al (2017) The effect of current *Schistosoma mansoni* infection on the immunogenicity of a candidate TB vaccine, MVA85A, in BCG-vaccinated adolescents: An open-label trial. PLoS Negl Trop Dis 11(5):e0005440
20. Brown J, Baisley K, Kavishe B, Changalucha J, Andreasen A, Mayaud P et al (2014) Impact of malaria and helminth infections on immunogenicity of the human papillomavirus-16/18 AS04-adjuvanted vaccine in Tanzania. Vaccine 32(5):611–617
21. Egwang TG, Owalla TJ, Kemigisha M (2022) COVID-19 vaccine trials must include helminth-infected cohorts. Nat Immunol 23(2):148
22. Su J, Hamway Y, Mistretta D, Liao B-H, Ma Z, Schluckebier J et al (2026) Helminth infection modulates the immunogenicity of COVID-19 vaccines in mice without compromising protective efficacy. Front Immunol 17:1827532
23. Desai P, Karl CE, Ying B, Liang CY, Garcia-Salum T, Santana AC et al (2024) Intestinal helminth infection impairs vaccine-induced T cell responses and protection against SARS-CoV-2 in mice. Sci Transl Med 16(761):eado1941
24. McCormack MJ, Banda L, Kasenda S, Samikwa L, Meleke H, Hughes EC et al (2026) Association between helminth infection and impaired SARS-CoV-2 antibody responses following COVID-19 vaccination: a cross-sectional study in Malawi. Sci Rep 16(1):26324
25. Niu M, Mu Y, Adriko M, Candia R, Jones MK, McManus DP et al (2024) COVID-19 vaccination survey and anti-SARS-CoV-2 IgG responses in a human cohort from *Schistosoma mansoni*-endemic villages in Mayuge District, Uganda: a cross-sectional study. Front Public Health 12:1437063
26. Cai P, Gobert GN, You H, Duke M, McManus DP (2015) Circulating miRNAs: Potential Novel Biomarkers for Hepatopathology Progression and Diagnosis of Schistosomiasis Japonica in Two Murine Models. PLoS Negl Trop Dis 9(7):e0003965
27. Rawle DJ, Le TT, Dumenil T, Yan K, Tang B, Nguyen W et al (2021) ACE2-lentiviral transduction enables mouse SARS-CoV-2 infection and mapping of receptor interactions. PLoS Pathog 17(7):e1009723
28. Mu Y, Yan K, McManus DP, Nguyen W, Rawle DJ, Roberts JA et al (2025) Marginal cytokine modulation by *Schistosoma mansoni* soluble egg antigen in SARS-CoV-2-infected K18-hACE2 mice. Folia Parasitol. ;72
29. Bishop CR, Dumenil T, Rawle DJ, Le TT, Yan K, Tang B et al (2022) Mouse models of COVID-19 recapitulate inflammatory pathways rather than gene expression. PLoS Pathog 18(9):e1010867
30. Andrews S (2010) A quality control tool for high throughput sequence data. Available online: https://www.bioinformatics.babraham.ac.uk/projects/fastqc
31. Li B, Dewey CN (2011) RSEM: accurate transcript quantification from RNA-Seq data with or without a reference genome. BMC Bioinformatics 12:323
32. Krämer A, Green J, Pollard J Jr, Tugendreich S (2014) Causal analysis approaches in ingenuity pathway analysis. Bioinformatics 30(4):523–530

33. Tang D, Chen M, Huang X, Zhang G, Zeng L, Zhang G et al (2023) SRplot: A free online platform for data visualization and graphing. PLoS ONE 18(11):e0294236
34. García-Bernalt Diego J, Desai P, Yeung ST, Damani-Yokota P, Khanna KM, Diamond MS et al (2025) Helminth infections affect host immune responses to viral infections and vaccines. FEMS Microbiol Rev 49:fuaf036
35. Su J, Hamway Y, Mistretta D, Liao B-H, Ma Z, Schluckebier J et al (2026) Helminth infection modulates the immunogenicity of COVID-19 vaccines in mice without compromising protective efficacy. Front Immunol 17:1827532
36. Musaigwa F, Kamdem SD, Mpotje T, Mosala P, Abdel Aziz N, Herbert DBR et al (2022) *Schistosoma mansoni* infection induces plasmablast and plasma cell death in the bone marrow and accelerates the decline of host vaccine responses. PLoS Pathog 18(2):e1010327
37. Nazeri S, Zakeri S, Mehrizi AA, Sardari S, Djadid ND (2020) Measuring of IgG2c isotype instead of IgG2a in immunized C57BL/6 mice with *Plasmodium vivax* TRAP as a subunit vaccine candidate in order to correct interpretation of Th1 versus Th2 immune response. Exp Parasitol 216:107944
38. Martin RM, Brady JL, Lew AM (1998) The need for IgG2c specific antiserum when isotyping antibodies from C57BL/6 and NOD mice. J Immunological Methods 212(2):187–192
39. Sahin U, Muik A, Derhovanessian E, Vogler I, Kranz LM, Vormehr M et al (2020) COVID-19 vaccine BNT162b1 elicits human antibody and TH1 T cell responses. Nature 586(7830):594–599
40. Wu Y, Zhang H, Meng L, Li F, Yu C (2022) Comparison of Immune Responses Elicited by SARS-CoV-2 mRNA and Recombinant Protein Vaccine Candidates. Front Immunol 13:906457
41. Costain AH, Phythian-Adams AT, Colombo SAP, Marley AK, Owusu C, Cook PC et al (2022) Dynamics of Host Immune Response Development During *Schistosoma mansoni* Infection. Front Immunol 13:906338
42. Hoffmann KF, Cheever AW, Wynn TA (2000) IL-10 and the dangers of immune polarization: excessive type 1 and type 2 cytokine responses induce distinct forms of lethal immunopathology in murine schistosomiasis. J Immunol 164(12):6406–6416
43. Yamaguchi Y, Kato Y, Edahiro R, Søndergaard JN, Murakami T, Amiya S et al (2022) Consecutive BNT162b2 mRNA vaccination induces short-term epigenetic memory in innate immune cells. JCI Insight. ;7(22)
44. Laidlaw BJ, Ellebedy AH (2022) The germinal centre B cell response to SARS-CoV-2. Nat Rev Immunol 22(1):7–18
45. Mu Y, Zumuk CP, Jones MK, Cai P (2026) Leveraging single-cell RNA-seq in helminthology. Trends Parasitol 42(1):61–74
46. Hosseini ST, Mahmanzar M, Rahimian K, Bayat S, Gholamzad A, Sisakht MM et al (2025) Spatial Transcriptomics and Single Cell-RNASeq Reveals Cellular Heterogeneity of SARS-CoV-2 in Lung Tissues and Global Mutational Patterns in COVID-19 Patients. J Med Virol 97(9):e70586

Figures

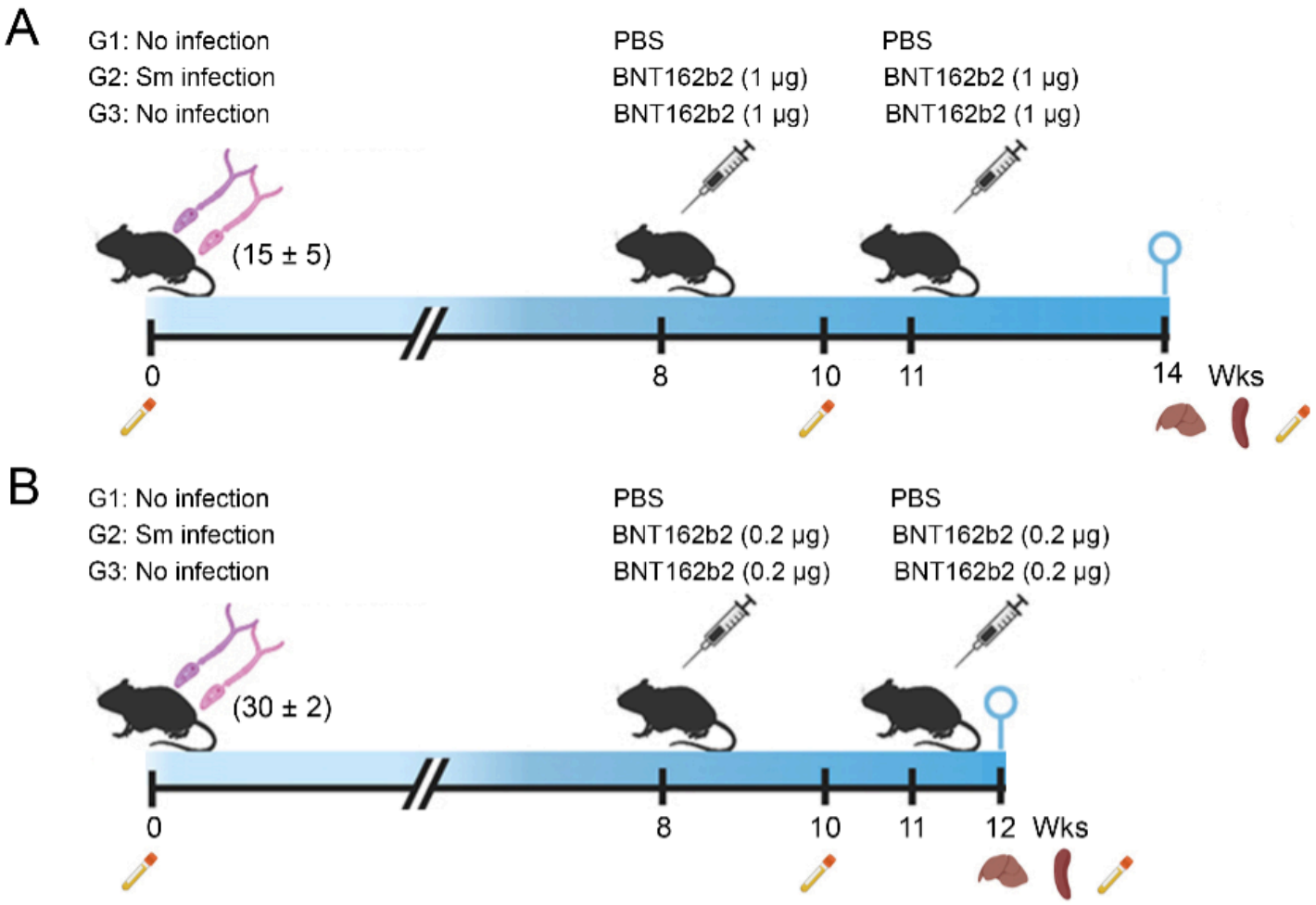


Figure 1

Schematic depiction of experimental designs. (A) Experiment 1 (Exp 1): C57BL/6J mice in Group 1 (G1) served as uninfected, unvaccinated controls and received PBS. Group 2 (G2) mice were infected percutaneously with a low number of *S. mansoni* cercariae (15 ± 5), while Group 3 (G3) remained uninfected. At 8 weeks post-infection, G2 and G3 mice were immunized intramuscularly with two doses of BNT162b2 (1 µg/mouse) at weeks 8 and 11. Serum samples were collected at week 0, 10 and 14, respectively. Mice were euthanised at 3 weeks after the booster immunisation (week 14) to assess vaccine-induced immune responses. (B) Experiment 2 (Exp 2): The experimental design was similar to Exp 1, except that G2 mice received a higher cercarial number (30 ± 2), and G2 and G3 mice were intramuscularly vaccinated with a lower dose of BNT162b2 (0.2 µg/mouse) at weeks 8 and 11. Serum samples were collected at the weeks 0, 10 and 12. Mice were euthanised at 1 week after the booster immunisation (week 12) to assess vaccine-induced immune responses. Figure created using BioRender (https://www.biorender.com/).

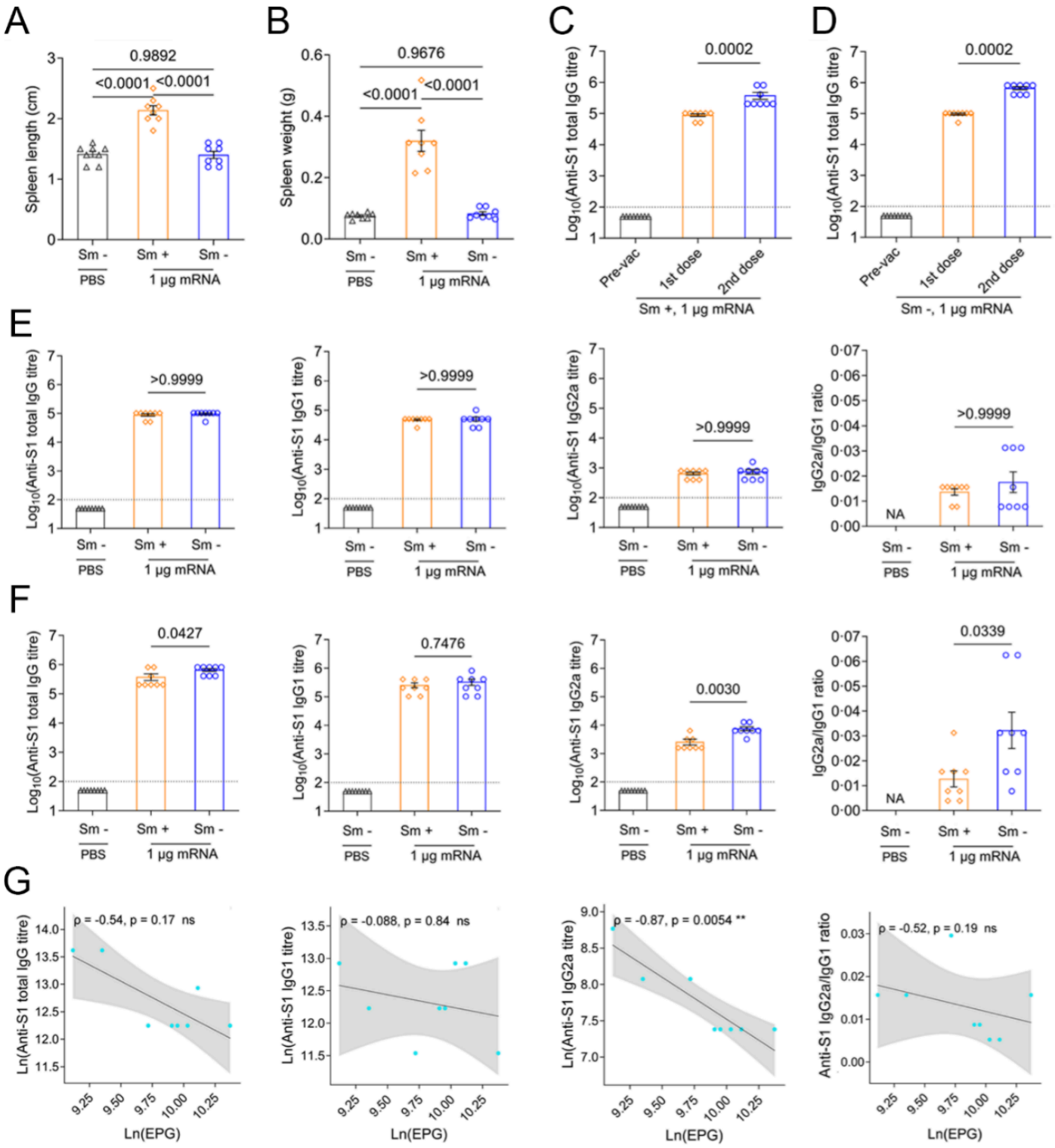


Figure 2

Comparison of serum IgG and IgG subclasses response of mRNA vaccine between *Sm*-infected and non-infected mice of Exp 1. **A)** Spleen length; **B)** Spleen weight. **C-D**) Total IgG response following first and second immunization in *Sm*-infected mice (**C**) and non-infected mice (**D**). **E)** Serum SARS-CoV-2 spike-specific IgG, IgG1, IgG2a, and IgG2a/IgG1 ratio at 2 weeks following the first immunization. **F)** Serum SARS-CoV-2 spike-specific IgG, IgG1, IgG2a, and IgG2a/IgG1 ratio at three weeks following the second

immunization. **G**). Correlations between liver egg burden and IgG, IgG1, and IgG2atitres as well as IgG2a/IgG1 ratio. Data are presented as mean ± SEM. Differences in spleen length and weight between groups were determined using the Kruskal–Wallis test. Differences in anti-S1 specific antibody titer and IgG2a/IgG1 ratio were determined using the Mann–Whitney *U* test. IgG2a/IgG1 ratio was defined as the maximum titer of IgG2a divided by maximum titer of IgG1.

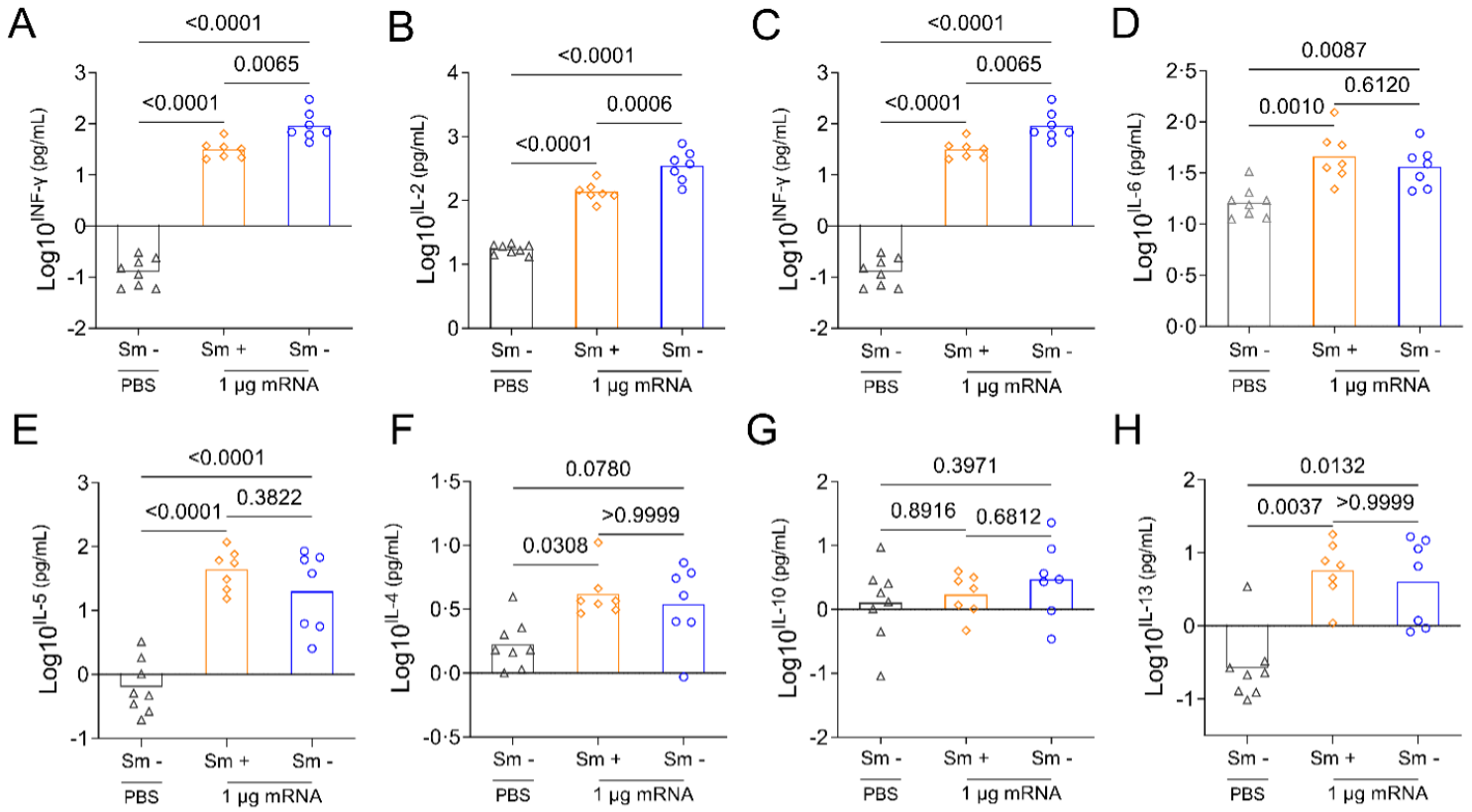


Figure 3

Comparison of splenic cytokine levels following stimulation between *Sm*-infected and non-infected mice of Exp 1. Cytokines **A**) IFN-γ, **B**) IL-2, **C**) TNF-α, **D**) IL-6, **E**) IL-5, **F**) IL-4, **G**) IL-10, and **H**) IL-13, secreted into the supernatants of splenocytes following stimulation with PepTivator SARS-CoV-2 Peptide Pools were detected using a LEGENDplex MU Th1/Th2 Panel (8-plex) w/VbP V03 kit. Differences in cytokine levels between groups were determined using one-way ANOVA or the Kruskal–Wallis test, as appropriate. (n = 8 for Group 1, n = 7 for Group 2, n = 7 for Group 3).

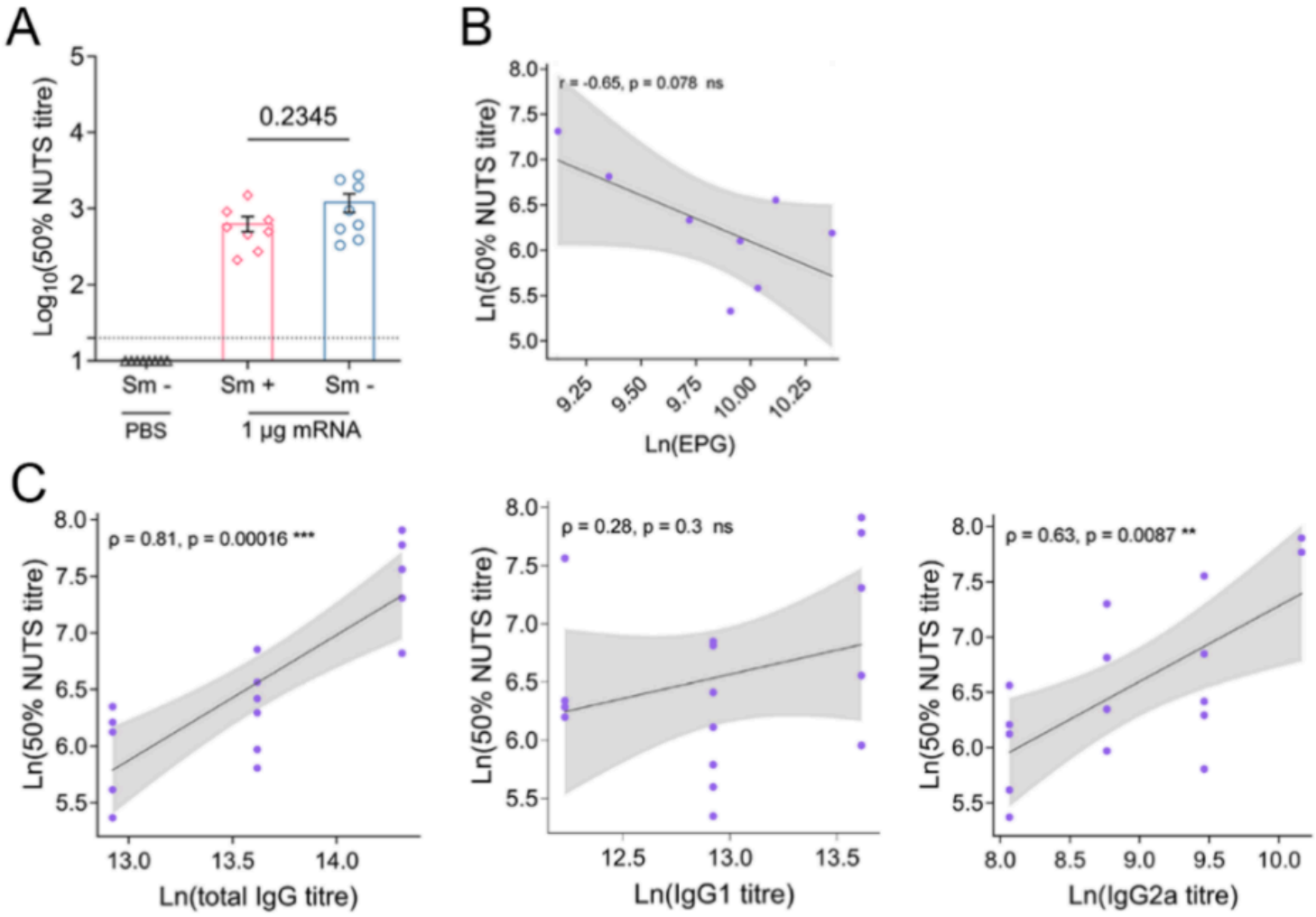


Figure 4

Serum neutralizing antibody titres for SARS-CoV-2 (Wuhan original strain) in vaccinated mice from Exp 1 at week 3 post the second immunization. A) Serum neutralizing antibody titres represented by IC_{50}. **B**) Correlations between liver egg burden and IC_{50} titre. **C**) Correlations between IC_{50} titres and IgG, IgG1, and IgG2a antibody titres. Panel A, data are presented as mean ± SEM. Differences in titre levels were determined using the Mann–Whitney *U* test.

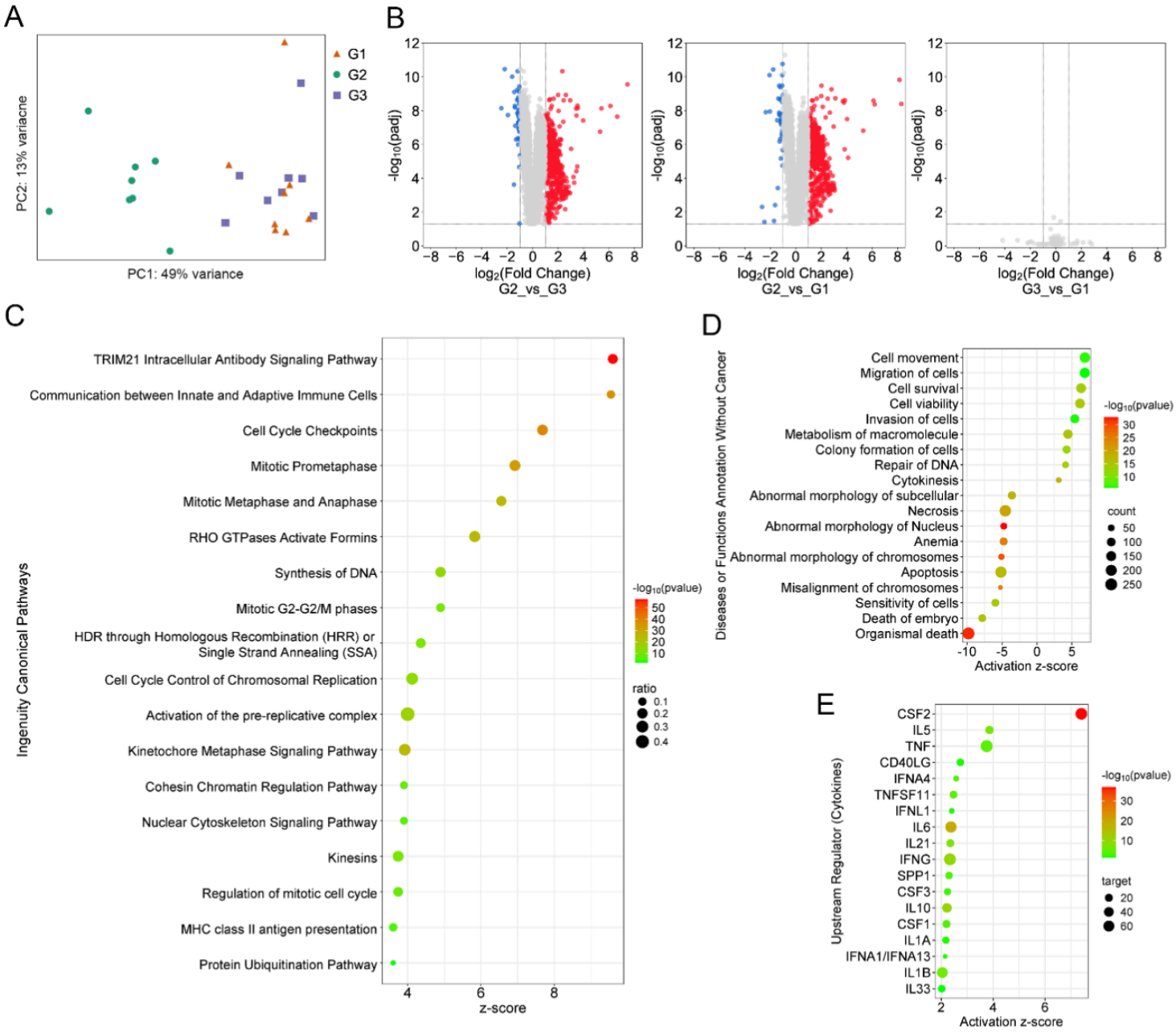


Figure 5

Bulk RNA-seq of spleen tissue. Spleen tissues were collected from three groups of mice of Exp 1 at week 14 (n = 8 mice per group). (A) Principal components analysis of total read counts. Points represent individual replicates. Each point represented an individual biological replicate, with samples colored according to experimental group. (B) Volcano plots of differentially expressed protein-coding genes between different groups. Red dots indicate significantly up-regulated DEGs, blue dots indicate significantly down-regulated DEGs, and gray dots represent not significantly DEGs. (C-E) Ingenuity Pathway Analysis (IPA, v84978992) of splenic DEGs between the infected, vaccinated group (G2) and the non-infected, vaccinated group (G3), identified using edgeR. (C) Ingenuity Canonical Pathways analysis. Pathways with z-scores greater than 3.5 were selected to present. (D). Diseases or Functions Annotations analysis. Annotations with z-scores greater than 3 or less than -3 were selected. Cancer-

related annotations were excluded. (E) Cytokines identified as upstream regulators. All genes presented had an overlap *p* value < 0.05. G1: Group 1, non-infected PBS control; G2: Group 2, infected vaccinated group; G3: Group 3, non-infected vaccinated groups.

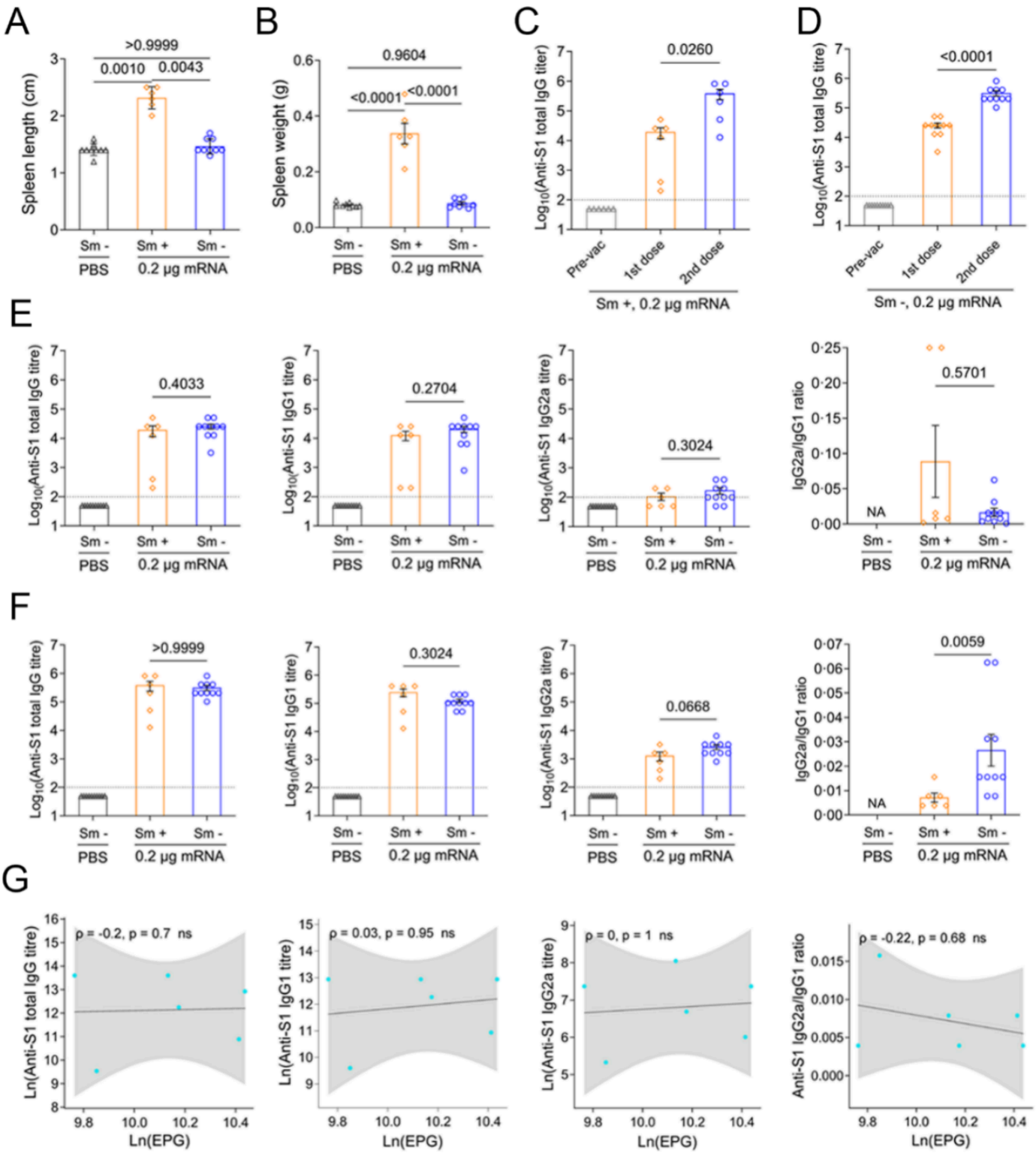


Figure 6

Comparison of serum IgG and IgG subclasses response of mRNA vaccine between *Sm*-infected and non-infected mice of Exp 2. **A)** Spleen length; **B)** Spleen weight. **C-D**) Total IgG response following first and second immunization in *Sm*-infected mice (**C**) and non-infected mice (**D**). **E)** Serum SARS-CoV-2 spike-specific IgG, IgG1, IgG2a, and IgG2a/IgG1 ratio at 2 weeks following the first immunization. **F)** Serum SARS-CoV-2 spike-specific IgG, IgG1, IgG2a, and IgG2a/IgG1 ratio at 1 week following the second immunization. **G**). Correlations between liver egg burden and IgG, IgG1, and IgG2atitres as well as IgG2a/IgG1 ratio. Panel A-F, data are presented as mean ± SEM Differences in spleen length and weight were determined using the Kruskal–Wallis test. Differences in anti-S1 specific antibody titer and IgG2a/IgG1 ratio were determined using the Mann–Whitney *U*test. IgG2a/IgG1 ratio was defined as the maximum titer of IgG2a divided by maximum titer of IgG1.

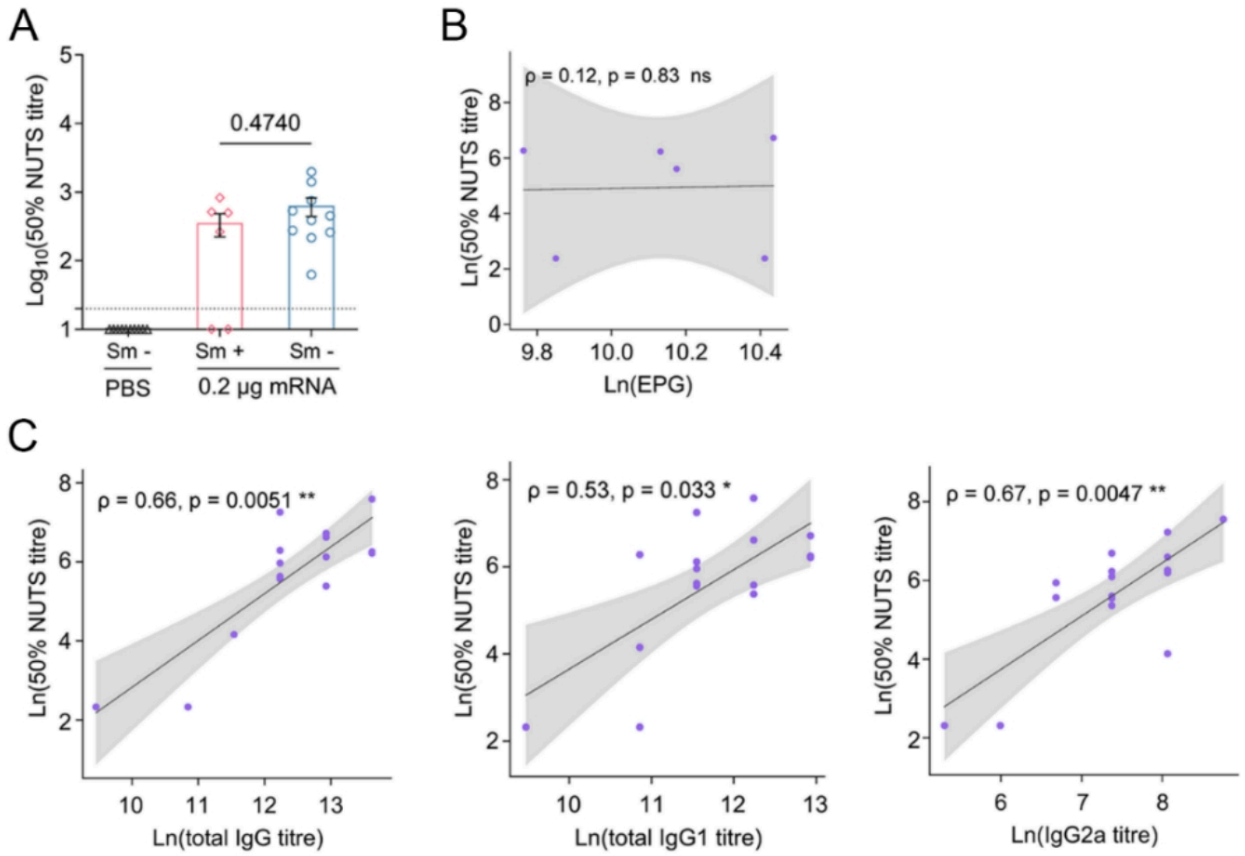


Figure 7

Serum neutralizing antibody titres for SARS-CoV-2 (Wuhan original strain) in vaccinated mice from Exp 2, measured one week after the second immunisation. A) Serum neutralizing antibody titres represented by IC_{50}. **B**) Correlations between liver egg burden and IC_{50} titre. **C**) Correlations between IC_{50} titres and total

spike-specific IgG, IgG1, and IgG2a antibody titres in all vaccinated mice. Panel A, data are presented as mean ± SEM. Differences in titre levels were determined using the Mann–Whitney *U* test.

Supplementary Files

This is a list of supplementary files associated with this preprint. Click to download.

- SupplementaryFigures.docx